17th World Conference on Earthquake Engineering, 17WCEE
Sendai, Japan - September 13th to 18th 2020

Seismic Fragility Assessment and Performance Evaluation of Structures based on a Grid Analysis Scheme

M. Sfahani[(1)], M. Kusz[(2)]

[(1)] *Senior Structural Engineer, KUSCH Consulting Engineers, mimo@kuschgroup.com.au*
[(2)] *Principal, KUSCH Consulting Engineers, martin@kuschgroup.com.au*

Abstract

Fragility curves are practical tools for seismic risk and damage vulnerability assessments of structures. Developing analytical fragility functions based on time-history analysis (THA) of nonlinear structural models has received extensive attention and application during the last decade, thanks to the feasibility of faster and more complex numerical computations. However, despite the availability of novel methods for developing such functions, incremental dynamic analysis (IDA) has remained the primary technique used for this purpose. This paper critically reviews the IDA method and explores its shortcomings when used to develop seismic fragility function, in terms of collapse intensity measures (IM), dispersion of non-collapse engineering demand parameters (EDP) of individual IDA curves and ground motion record (GMR) scaling. Providing exceptional and specific recommendations to overcome these shortcomings, a grid analysis scheme (GAS) is developed for seismic fragility assessments of structures based on THA. The GAS technique begins with Cloud analysis and assessing the adequacy of sampled datapoints for representing structural collapse and considered performance levels. The THA realisations of the structural model is then continued and the general closed form solution to the analytical fragility function can be determined by as low as two additional specific THA per each selected GMR.

Keywords: Analytical fragility function; Time-history analysis; Ground motion record scaling; Seismic data gridline

1. Introduction

Seismic fragility analysis is a fundamental step in modern performance-based earthquake engineering (PBEE) [1]. The structural seismic fragility is defined in terms of the conditional probability (P) of exceeding a limit-state (LS), for a given earthquake intensity measure (IM). The LS herein is a nominated structural response threshold in terms of an engineering demand parameter (EDP), e.g. deformation or force, to represent a predefined structural performance (i.e. a damage) level [2]. This analysis generates fragility curves, indicating structures' seismic vulnerability, as the envelopes of failure probability increase with increasing IMs [3]. A fragility curve is shown in Fig.1 schematically.

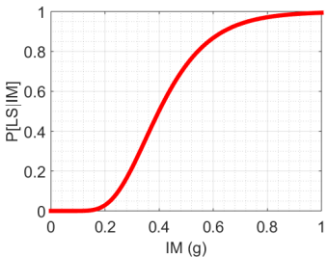

Fig. 1 – Schematic example of a fragility curve [2]

Although fragility curves can be generated based on empirical seismic data [4] or experts' opinion [5], analytical fragility functions [6] have become the primary tool for this purpose:

$$P[LS|IM] = G_{EDP|IM,NC}(LS|IM) \cdot P_{NC|IM} + G_{EDP|IM,C}(LS|IM) \cdot P_{C|IM} \quad (1)$$

where G(·) is the complementary cumulative density function (CDF) of the estimated EDPs (with respect to the specified LS) and $P_{C|IM}$ denotes the conditional collapse probability given IM. These functions rely on numerical simulation of structures subjected to earthquake loads. Various numerical techniques have been developed to establish the analytical fragility functions such as the capacity spectrum method [7], multiple stripe analysis [8], incremental dynamic analysis (IDA) [9] and Cloud analysis [10], Cloud to IDA (CIDA) [11], and extended Cloud analysis (ECA) [12]. The differences between these techniques are the integrity in simulation, efficiency of computation and versatility in application [2]. In terms of the integrity of simulation earthquake loads, methods which are established on the time-history analysis (THA) have gained more attention in the last decade, thanks to the feasibility of faster numerical computations. In this regard, the original Cloud analysis (addressed as OCA in the rest of this text) and the IDA are recognised as the basic and the most rigorous techniques, respectively.

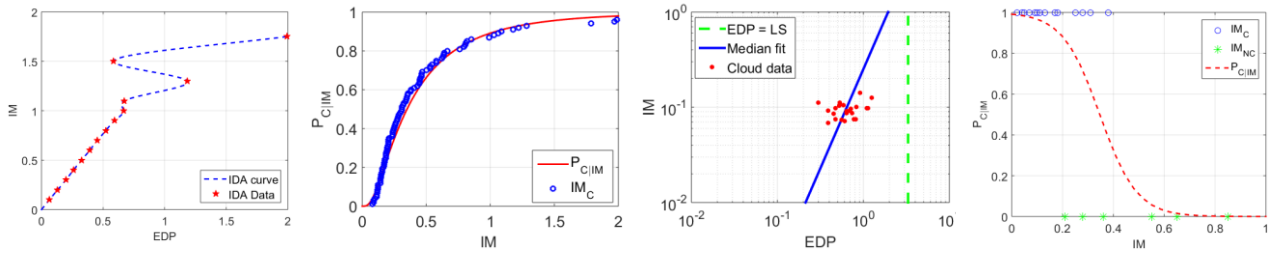

(a) Single IDA (b) IDA curve fitting (c) Cloud of sampled data (d) Logistic regression

Fig. 2 – Schematic data sampling and regression analysis for IDA and OCA methods [2]

OCA and IDA have both similarities and differences, which can be used to distinguish their advantages and disadvantages. For example, both methods utilise a lognormal distribution for a sampled seismic dataset (IM–EDP) and give a closed-form solution to Eq. (1), as follows:

$$P[LS|IM] = \Phi^{C}_{EDP|IM,NC}\left(\frac{\log LS - \log \eta_{EDP_{NC}|IM}}{\beta_{EDP_{NC}|IM}}\right) \cdot (1 - P_{C|IM}) + P_{C|IM} \quad (2)$$

where Φ^C is the standardised Gaussian (normal) CDF of non-collapse sampled seismic dataset $(IM–EDP)_{NC}$ and η and β are respectively the median and standard deviation (from the median) of lognormal distribution (of this dataset). Comparatively, the most significant difference between the OCA and IDA methods is their computational efficiency. OCA can be conducted by performing as few as a single THA for each ground motion record (GMR) selected for the seismic fragility study. In other words, each IM–EDP datapoint (solid red circles) in Fig.2(c) represents a THA conducted using a GMR selected for the study. However, when using the IDA method, THA is conducted repeatedly, for different derivatives of a GMR, scaled linearly up until the identification of the minimum collapse intensity measure (IM_C) for that GMR. Subsequently, a curve is generated by spline curve fitting to the sampled IM–EDP dataset for each GMR in the study (see Fig.2(a)). This also allows the generation of an empirical CDF using identified IM_C via IDA, which a curve can be fitted to (see Fig.2(b)) for evaluation of $P_{C|IM}$.

This increases the computational costs dramatically since no definite provision can be set to ensure the identification of IM_C for all GMRs in the study, using a limited number of THA. This difference between the two techniques implies a distinction in the parameter β as calculated by OCA and IDA, as the former gives it as a constant, while the latter determines it to be varying as a function of IM, i.e. $\beta_{EDP|IM}$. This distinction has been found to be one source of inaccuracy of the OCA method when IM increases [12]. Additionally, despite the availability of GMR selection techniques for THA, such as conditional mean spectrum (CMS) [13] and conditional spectrum (CS) [14], the only current method to utilise with OCA is the conventional filtering

method. This is because, in the absence of scaled derivatives of selected GMRs in the OCA method, the sampled IM–EDP dataset becomes highly sensitive to the selection criteria, which can lead to the constant β parameter becoming even lower. However, adopting a filtering GMR selection can create other shortcomings such as an inappropriate cloud of IM–EDP dataset for the coverage of a performance LS. Such an observation, as shown schematically in Fig.2(c), simply indicates the inadequacy of sampled data for reflecting the seismic fragility of structures with respect to considered performance, LS. Moreover, the logistic regression, which is conducted to determine $P_{C|IM}$ in the OCA method, is extremely susceptible to the binary distribution of IM_C and IM_{NC}. For example, see Fig.2(d) and how $P_{C|IM}$ decreases as IM increases.

Although it reveals that IDA is a more versatile method than OCA in terms of application, there are a couple of ambiguities with the application of IDA method [9]. IDA requires determination of the medians of sampled IM–EDP datapoints for individual GMRs, which are then averaged to evaluate η of the entire dataset. Within this process, the dispersion of IM–EDP datapoints with respect to the median fit of individual GMRs is eliminated. This elimination insets an unnecessary uncertainty, which is ignored in developing the analytical frailty function based on the IDA method. The other issue is the collapse criteria utilised by the IDA method. In general, for a given GMR, the occurrence of collapse during THA can be defined in several ways [15]. For IDA, these include reaching a local gradient of 20% of the elastic slope over the IDA curve, numerical non-convergence, and setting an upper EDP bound. Numerical experiments show tracking the local gradient of IDA curves is not always feasible and/or valid for different structural models and pattern-timing of the scaled GMRs due to natural period elongation [2]. In addition, this theoretical collapse criterion has never been validated by experimental testing. Furthermore, there is ongoing research into overcoming the numerical non-convergence issues under large displacements and corresponding deformations, [16] which questions the credibility of this assumption as a valid collapse criterion. Consequently, only the adoption of an EDP bound e.g., exceedance of a drift threshold, can be justified (based on theory, numerical study or experiment) as a collapse criterion for IDA.

This paper proposes a grid analysis scheme (GAS) for seismic fragility analysis in order to overcome the aforementioned shortcomings of OCA and IDA. The GAS method can be conducted using as few as three THA realisations of a numerical or analytical structural model for each selected GMR for the study. An important advantage of the GAS technique which makes it appealing for PBEE is that it is correlated to predefined seismic damage and structural performance levels under investigation. This correlation is initially triggered by application of OCA and is preserved stepwise through the GAS process. It is worth noting that the GAS technique has substantial differences from the existing ECA and CIDA methods, despite all using OCA in the first step, which makes it a novel technique with distinct advantages over these methods. In the following, the GAS technique concept and its formulation for developing seismic fragility analysis is detailed.

2. Grid Analysis Scheme Methodology

2.1 Grid of structural performance

The OCA is a key THA–based method for seismic fragility analysis and is an opening to PBEE. Following the completion of OCA, η and β can be determined through a linear regression in logarithmic space for sampled $(IM–EDP)_{NC}$ datapoints, and $P_{C|IM}$ is evaluated through logistic regression of sampled $IM_C–IM_{NC}$. In other words, it is assumed the sampled $(IM–EDP)_{NC}$ datapoints are distributed lognormally [6] while a binary function holds the distribution of sampled $IM_C–IM_{NC}$ [17]. At this stage, and before proceeding to develope the closed-form solution (i.e. Eq. (2)), it is crucially important to examine the adequacy of sampled datasets in terms of representing the considered structural performance levels. A tool for such an examination can be a grid of structural performance LS lines as shown in Fig.3. This can be generated by plotting the EDP upper bound corresponding to structural collapse (i.e. EDP = C) as well as all other EDP bounds corresponding to considered structural performance levels (i.e. EDP = LS) for seismic fragility analysis. Note that in addition to collapse, only a single performance level is considered in Fig.3, which divides the sampling space into the linear (EDPs < LS), nonlinear (LS ≤ EDPs < C) and collapse responses (EDPs ≥ C). All EDPs ≥ C are also mapped on the EDP = C line for the purpose of illustration. Moreover, the IM levels corresponding to EDP =

LS (i.e. IM_{LS}) and EDP = C (i.e. IM_C) should be determined using the $\eta_{EDP|IM}$ function and plotted in the sampling space.

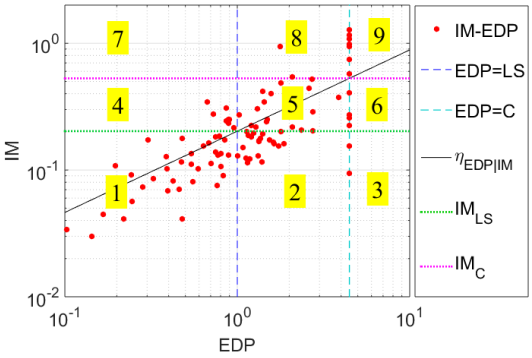

Fig. 3 – A grid of structural performance (schematic)

Subsequently, the sampling space is subdivided into n^2 new subspaces (i.e. 1–9 in Fig.3), where n is the number of considered performance levels plus two. This new subdivided space allows to determine if the sampled dataset is adequate for fragility analysis with respect to considered structural performance levels and collapse. For example, to generate reliable seismic fragility curves based on OCA, the sampled datapoints should cover different EDP subspaces evenly. However, this is not possible to guarantee a priori due to GMR randomness issues, unless GMRs are selected quite subjectively. Also, the datapoints could be ideally distributed in the subspaces 1 (linear EDPs), 5 (nonlinear EDPs) and 9 (collapse cases), in the vicinity of estimated $\eta_{EDP|IM}$, although this is quite unlikely due to structural nonlinear behaviour and period elongation issues. Under these circumstances, a solution can be to introduce extra GMRs for the OCA, particularly when instable logistic regression issues occur. However, this is again subjective and can give biased fragility results. The substitute solution, herein, is walking toward an alternative fragility analysis method using scaled derivatives of originally selected GMRs. In this case, the fundamental question becomes how to scale the GMRs. This is described in the next section.

2.2 Information-based GMR scaling

Four information-based approaches have been proposed by Sfahani [2] for scaling selected GMRs based on initial OCA results. These are briefly described in the following.

2.2.1 Stripe scaling approach

Stripe scaling approach (SSCA) involves scaling a GMR to a specific IM level. A stripe of EDPs can be achieved in case all selected GMRs are scaled to a given IM level. This IM level can be determined to represent a specific structural performance level as follows

$$IM_{SSCA} = \sqrt[b]{\frac{LS}{a}} \tag{3}$$

where LS is the numerical EDP value representing the considered performance level, and a and b are the intercept and slope of linear median fit ($\eta_{EDP|IM}$) in logarithmic space, respectively (see Fig.4(a)).

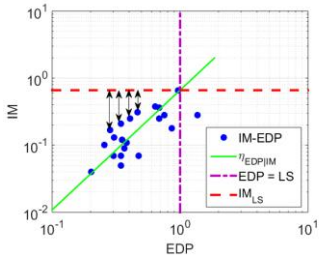

(a) Stripe scaling approach (SSCA)

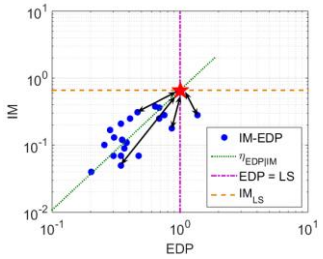

(b) Transition scaling approach (TSCA)

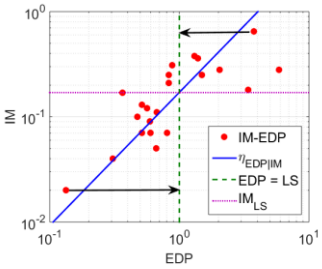

(c) Mapping scaling approach (MSCA)

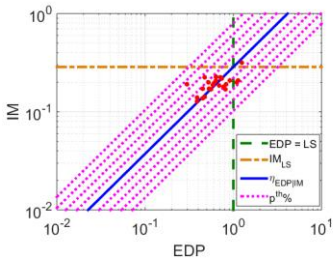

(d) Percentile scaling approach (PSCA)

Fig. 4 – Information-based GMR scaling approaches [2]

2.2.2 Transition scaling approach

An IM–EDP datapoint can be shifted toward a specific performance spot in the sampling logarithmic space. This is called transition scaling approach (TSCA), which is schematically shown in Fig.4(b). The scale factor (SF) for the GMR_i can be determined as follows

$$SF_{TSCA} = \sqrt{\left(\frac{IM_{LS}}{IM_i}\right)^2 + \left(\frac{LS}{EDP_i}\right)^2} \tag{4}$$

where IM_i and EDP_i correspond to the IM–EDP response obtained by GMR_i, and LS and IM_{LS} are numerical values representing the considered performance level.

2.2.3 Mapping scaling approach

GMRs can be mapped to meet a structural performance level (see Fig.4(c)). This is called the mapping scaling approach (MSCA), which is similar to SSCA. However, the obtained EDP is used to calculate SF for GMR_i. The SF can be simply determined as follows

$$SF_{MSCA} = \frac{LS}{EDP_i} \tag{5}$$

where EDP_i corresponds to the response obtained by GMR_i, and LS is the numerical values representing the considered performance level.

2.2.4 Percentile scaling approach

The closed-form solution to the analytical fragility function (i.e. Eq. (2)) utilises the median (i.e. 50% probability) of distribution of IM–EDP datapoints (i.e. $\eta_{EDP|IM}$) to evaluate a different confidence bound of

seismic fragility, through which the corresponding percentile p^{th} can be utilised (see Fig.4(d)). The percentile scaling approach (PSCA) is to scale the original GMRs to the sorted IMs which cover a specific structural performance level. To this end, the IM percentile for GMR_i, for a given performance level can be approximated as follows

$$IM_{PSCA} = \sqrt[b]{\frac{IM_i^b \cdot LS}{EDP_i}} \tag{6}$$

where IM_i and EDP_i correspond to the IM–EDP response obtained by GMR_i, LS is the numerical value representing the considered performance level and b is the slope of median fit ($\eta_{EDP|IM}$) in logarithmic space.

2.3 GAS technique–Stage 1

The number of THA required for seismic fragility analysis by the GAS technique is correlated with PBEE and the number of considered structural performance levels. In this regard, the suggested number of THA to be conducted for each selected GMR is n+2, where n is the number of performance levels. In this paper, in order to simply and clearly put the new GAS method forward, only a single performance level has been considered in addition to the collapse threshold. A more comprehensive and expanded GAS methodology with the inclusion of multiple structural performance levels will be described in future publications.

The first stage of GAS method is comprised of the classification and scaling of the IM–EDP datapoints sampled by OCA. Note that a grid of structural performance has already been generated in Fig.3, but a more detailed data classification needs to be conducted to scale each GMR individually. Additionally, the linear (1,4,7), nonlinear (2,5,8) and collapse (3,6,9) subspaces have been outlined (see Fig.3). It is worth reiterating that subspaces 1, 5 and 9 are on the mainstream. Further, the datapoints in subspaces 7 and 3 are classified as outliers and they are removed from the seismic fragility analysis. Identification and treatment of outliers in a regression analysis can be carried out in several ways [18]. In this situation, the treatment is based on the justification that the GMRs in subspace 7 produce linear responses while their IM levels are greater than IM_C and, the GMRs in subspace 3 produce collapse responses while their IM levels are lower than IM_{LS}. In general, the IM–EDP datapoints to the right of $\eta_{EDP|IM}$ line are stronger GMRs than those to the left of this line. This can be simply justified based on comparison of EDPs determined by these GMRs with the EDPs approximated via $\eta_{EDP|IM}$, for the same IM levels. As such, subspaces 4 and 2 are classified as the weak and strong GMRs, respectively. These GMRs are also deviated from $\eta_{EDP|IM}$ to some extent but they are maintained for the rest of analysis, since they can be brought back to the mainstream. Finally, datapoints in subspaces 8 and 6 are the most inelastic GMRs. Although it seems these GMRs display similar deviations to those in subspaces 4 and 2, the fact that subspaces 8 and 6 are not linear means that they cannot be treated in the same manner. However, these GMRs can remain in the analysis with some provisions.

The aim of the GAS technique in Stage 1 is to generate a pair of $(IM\text{-}EDP)_{NC}$ datapoints. As previously discussed, the dispersion of these datapoints is ignored for individual GMRs in the IDA method. In the GAS methodology, this dispersion is eliminated from the analysis by using only a pair of $(IM\text{-}EDP)_{NC}$ datapoints from linear regression in the logarithmic space. Consequently, as such a dispersion and related uncertainties are not generated, the complications from this can be disregarded. The proposed layout for GMR scaling at GAS–Stage 1 is illustrated in Fig.5. This layout targets the considered structural performance level by sampling additional IM-EDP datapoints in the vicinity of corresponding LS. For this purpose, the weak GMRs in subspace 1 (GMR_{1W}) and the strong ones in subspace 5 (GMR_{5S}) are sorted using PSCA to their corresponding percentiles on the EDP = LS line, using Eq. (6). Other GMRs in these subspaces (i.e. GMR_{1S} and GMR_{5W}) are striped to the IM_{LS} level by SSCA, using Eq. (3). Then, the GMRs in the subspaces 4 and 2 are mapped to the EDP = LS line (MSCA) and those in subspace 8 are shifted to the intersection of this line with IM_{LS} (TSCA) using Eq. (5) and Eq. (4), respectively.

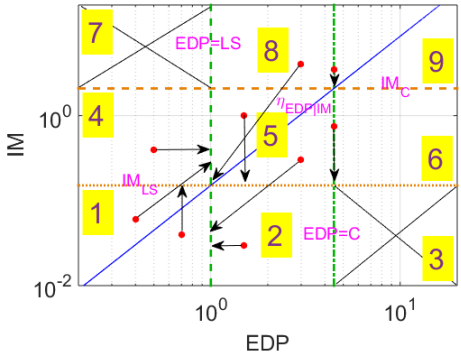

Fig. 5 – GMR scaling layout at Stage 1 of GAS technique (schematic)

Due to being collapse cases, the EDPs achieved by GMRs in subspaces 6 and 9 can be unrealistic, so they are mapped on the EDP = C line in Fig.5. There is no chance to sample a pair of $(IM\text{-}EDP)_{NC}$ for these GMRs at Stage 1 and therefore, GMR_6 and GMR_9 are inevitably scaled down to IM_{LS} and IM_C, respectively, awaiting for a pair of $(IM\text{-}EDP)_{NC}$ to be achieved at Stage 2.

2.4 GAS technique–Stage 2

The aim of the GAS technique at Stage 2 is to sample the IM_C levels of GMRs. Note that Stage 1 aimed to generate a pair of $(IM–EDP)_{NC}$ datapoints. Similar to stage one, it is first necessary to classify the dataset sampled in the former stage. Considering the assumptions of this study, nine feasible cases to be sampled by GAS–Stage 1 are summarised in Table 1. The GAS–Stage 2 treats each case separately.

Table 1 – Classification of sampled IM–EDP dataset; linear (L), nonlinear (N) and collapse (C) cases

Case	**1**	**2**	**3**	**4**	**5**	**6**	**7**	**8**	**9**
OCA	L	L	L	N	N	N	C	C	C
GAS–Stage 1	L	N	C	L	N	C	L	N	C

Case 1:

Although all linear datapoints are scaled up at GAS–Stage 1 to sample a nonlinear or collapse response, some GMRs may result in a second linear response. In this case, the GMR is scaled to the IM level at EDP = C for THA at GAS–Stage 2. If the slope of the linear regression by this pair of linear datapoints (b_i) was lower than the slope of existing line's (b_η), the GMR is scaled to the IM levels extrapolated by $\eta_{EDP|IM}$ at EDP = C. Otherwise, the linear regression found using the Case 1 datapoints is used to extrapolate the IM level at EDP = C. Then, if the new THA at GAS–Stage 2 did not sample a collapse response, all three sampled IM-EDP datapoints are utilised to determine the median of individual GMRs. IM_C is approximated by extrapolation at EDP = C but using the larger pair of sampled datapoints. The reason for these provisions is that a pair of linear datapoints is not adequate for an accurate extrapolation and, therefore it is necessary to be conservative in identifying the lowest IM_C for a GMR.

Case 2:

This case is more straightforward. Similar to Case 1, for the THA at GAS–Stage 2, GMRs are scaled to the IM levels extrapolated at EDP = C however, it uses the sampled pair of datapoints. This is because these datapoints indicate the scaling approach at GAS–Stage1 was successful and therefore this pair can be reliably

used for extrapolation. Similar to Case 1, if a collapse response was not sampled at GAS–Stage 2, the three IM-EDP datapoints can be used to determine the median of individual GMRs, and IM_C can be approximated by extrapolation at EDP = C using the pair of nonlinear datapoints.

Case 3:

In this circumstance, the GMRs are treated similarly to GAS–Stage 1 but, are scaled to a lower IM level at GAS–Stage 2. In this regard, GMR_{1W} and GMR_4 (see Fig.5) are striped to the IM_{LS} level using SSCA (Eq. (3)) and GMR_{1S} is sorted on the EDP = LS line using PSCA (Eq. (6)). An undesirable outcome in this case is sampling a second collapse response for these GMRs at GAS–Stage 2. This necessitates continuing THA for these GMRs by another SF, such as mapping the strong and weak GMRs to their corresponding IM and EDP levels on the $\eta_{EDP|IM}$ line. The IM_C in this case is the lower of all identified collapse responses.

Case 4:

This case is treated identically to Case 2.

Case 5:

This case is treated identically to Case 1.

Case 6:

This case may look similar to Case 3 but it should be noted that nonlinear datapoints at GAS–Stage 1 were scaled down to lower IM levels. As such, the occurrence of Case 6 can be interpreted as an error within the THA or the numerical/analytical model developed for the analysis. Alternatively, if there is enough confidence about the THA and model being used, a lower subjective SF can be utilised for these GMRs at GAS–Stage 1

Case 7:

In this case, the newly sampled linear datapoint can be treated similar to GMRs in subspace 4 at GAS–Stage 1, noting that the IM level determined at GAS–Stage 2 cannot be bigger than the IM_C identified for the GMR using OCA. If this is an issue, the provisions advised for Case 3 can be adopted.

Case 8:

This case is similar to Case 7, where the newly sampled nonlinear datapoint can be treated similarly to GMRs in subspaces 2 or 8 at GAS–Stage 1, depending on the IM level. GMRs can be scaled down confidently.

Case 9:

Finally, this is an undesirable case which indicates the THA must be repeated for these GMRs with more than one SF, up until sampling a pair of $(IM–EDP)_{NC}$. If this case occurred for GMRs in the subspace 9, the GMRs can be scaled down to the IM_{LS} (see Fig.5), and then the advised provisions for Cases 7 or 8 can be adopted as required. Otherwise, a lower subjective SF should be utilised. The IM_C for these GMRs is taken as the lowest of all identified collapse responses.

2.5 Seismic fragility analysis by GAS technique

The stepwise process for performing seismic fragility analysis based on the GAS technique is illustrated in Fig.6. The analysis can be conducted once as long as n+2 IM–EDP datapoints were sampled for each selected GMR. Note that to determine the intercept a_i and slope b_i of linear regression for an individual GMR in logarithmic scale, at least one pair of these datapoints must be a non-collapse case. Otherwise the analysis is continued at GAS–Stage 2 until this result is achieved. The lognormal median, $\eta_{EDP,NC|IM,}$ and standard deviation, $\beta_{EDP,NC|IM,}$ of the distribution of the entire dataset can be determined as they are for IDA, using following equations

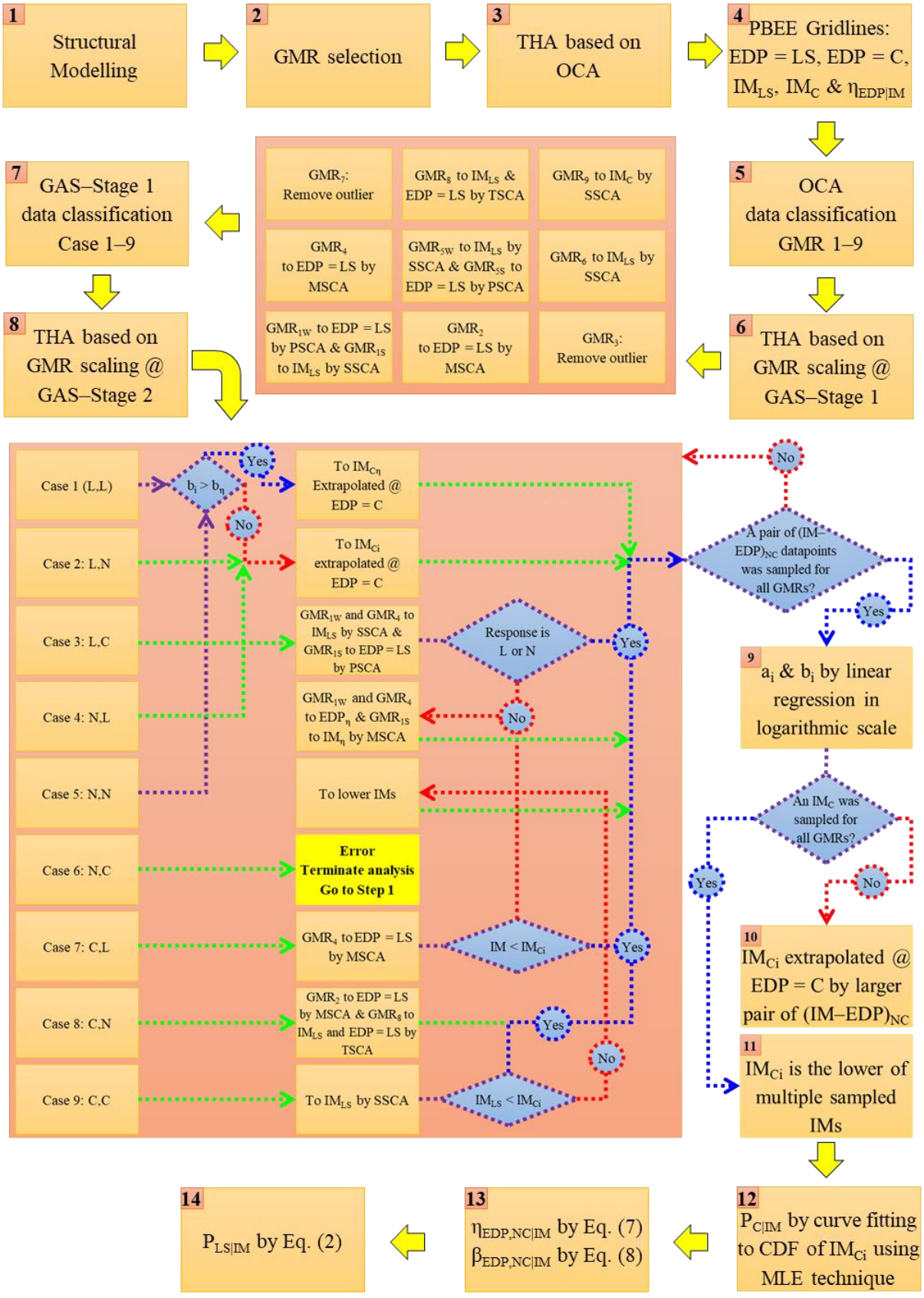

Fig. 6 –Seismic fragility analysis based on GAS technique

$$\eta_{EDP_{NC}|IM} = \eta_{a_i}\, IM^{\mu_{b_i}} \tag{7}$$

$$\beta_{EDP_{NC}|IM} = \sqrt{\sigma^2_{log\, a_i} + \sigma^2_{b_i}\, (\log IM)^2 + 2\, \rho\, \sigma_{b_i}\, \sigma_{log\, a_i}\, (\log IM)} \tag{8}$$

where η, μ, σ^2 and ρ are the median, mean, variance and coefficient of correlation of the a_i and b_i determined for different GMR_i. Additionally, the $P_{C|IM}$ can be determined by fitting a curve to the CDF of all IM_{Ci} values sampled for different GMR_i using the maximum likelihood technique (MLE) [8]. Subsequently, to determine the closed-form solution of analytical seismic fragility function based on the GAS technique, Eq. (7), Eq. (8) and $P_{C|IM}$ can be substituted into Eq. (2).

3. Discussion and Future Work

An OpenSees–MATLAB implementation of the proposed algorithm for the GAS technique will soon be available to download. A case study for numerical validation of this technique for seismic fragility analysis is also in progress and will be reported upon completion. In addition to these projects, an expanded GAS technique for inclusion of multiple structural performance levels in seismic fragility analysis is under development by the authors and will be published in future. Note that the closed–form solution obtained for fragility function in this paper (based on the present GAS technique) can also be utilised for the same purpose. However, as identified earlier, the reliability of resulting fragility curves become unclear when the dataset is not sampled to represent all performance levels.

Sampling extra datapoints for additional structural performance levels increases the number of required THA and thus the computational cost. Nevertheless, it is the versatility of the GAS methodology which motivates its application for seismic fragility analysis. Moreover, this increase is limited to one extra THA for each additional performance LS, per selected GMR, minimising the computational cost. Further studies which can be conducted in conjunction with the GAS technique are an analysis of sensitivity to GMR selection methods and ranking of different IMs and EDPs for GMR scaling. Additionally, assessing the sensitivity of seismic fragility results to uncertainties within the nominated LS bounds for GAS technique would be beneficial.

4. Conclusion

Seismic fragility analysis is as essential requirement for long-term performance prediction of structures. In this paper, the existing OCA and IDA methods have been reviewed critically and a novel analytical technique, called GAS, was proposed which eliminates the shortcomings of these methods. In particular the development of the GAS methodology has led to the following findings:

- The GAS technique is entirely correlated with the considered structural performance levels by sampling a dataset which well represents these levels, as well as structural collapse. This is done by approving the quality of the sampled dataset against the gridlines of PBEE.
- The GAS technique utilises non-subjective and specific GMR scaling approaches which treats each selected GMR individually. These approaches target the considered structural performance levels.
- Seismic fragility analysis based on the GAS technique can be conducted using as low as n+2 THA for each selected GMR, where n is the number of performance levels considered. The two additional THA are for the linear and collapse responses (one each) in the sampled dataset.
- The median of seismic responses for individual GMRs can be determined by using only a pair of $(IM\text{-}EDP)_{NC}$ datapoints in the GAS technique. This eliminates the generation of dispersion by these datapoints, decreases the uncertainties and elaborates the efficiency of computation by this technique.

- The GAS technique also eliminates the spline curve fitting process by using a pair of $(IM\text{-}EDP)_{NC}$ datapoints and recognises a sole collapse criterion, the EDP upper bound, for all selected GMRs.
- Using the GAS technique allows the determination of an IM_C level for all GMRs which can be used to generate a CDF with a fitted curve and eliminates the necessity of logistic regression.

5. References

[1] C. Cornell and H. Krawinkler. (2000) Progress and challenges in seismic performance assessment. *PEER Center News*. 1-3.
[2] M. Sfahani, "Seismic Fragility Assessment of Highway Overpasses with Pier Walls in Low-to-Moderate Seismic Zones," 2017.
[3] M. Sfahani, H. Guan, and Y.-C. Loo, "Seismic Reliability and Risk Assessment of Structures Based on Fragility Analysis–A Review," *Advances in Structural Engineering*, vol. 18, no. 10, pp. 1653-1669, 2015.
[4] M. Shinozuka, M. Q. Feng, J. Lee, and T. Naganuma, "Statistical analysis of fragility curves," *Journal of Engineering Mechanics*, vol. 126, no. 12, pp. 1224-1231, 2000.
[5] K. Porter, R. Kennedy, and R. Bachman, "Creating fragility functions for performance-based earthquake engineering," *Earthquake Spectra*, vol. 23, no. 2, pp. 471-489, 2007.
[6] C. Cornell, F. Jalayer, R. Hamburger, and D. A. Foutch, "Probabilistic basis for 2000 SAC federal emergency management agency steel moment frame guidelines," *Journal of Structural Engineering*, vol. 128, no. 4, pp. 526-533, 2002.
[7] P. Fajfar, "A nonlinear analysis method for performance-based seismic design," *Earthquake spectra*, vol. 16, no. 3, pp. 573-592, 2000.
[8] J. W. Baker, "Efficient analytical fragility function fitting using dynamic structural analysis," *Earthquake Spectra*, vol. 31, no. 1, pp. 579-599, 2015.
[9] D. Vamvatsikos and C. Cornell, "Incremental dynamic analysis," *Earthquake Engineering & Structural Dynamics*, vol. 31, no. 3, pp. 491-514, 2002.
[10] F. Jalayer, "Direct probabilistic seismic anaysis: implementing non-linear dynamic assessments," PhD, Stanford University, 2003.
[11] A. Miano, F. Jalayer, H. Ebrahimian, and A. Prota, "Cloud to IDA: Efficient fragility assessment with limited scaling," *Earthquake Engineering & Structural Dynamics*, vol. 47, no. 5, pp. 1124-1147, 2018.
[12] M. Sfahani and H. Guan, "An extended cloud analysis method for seismic fragility assessment of highway bridges," *Earthquakes and Structures*, vol. 15, no. 6, pp. 605-616, 2018.
[13] J. W. Baker, "Conditional mean spectrum: Tool for ground-motion selection," *Journal of Structural Engineering*, vol. 137, no. 3, pp. 322-331, 2010.
[14] N. Jayaram, T. Lin, and J. W. Baker, "A computationally efficient ground-motion selection algorithm for matching a target response spectrum mean and variance," *Earthquake Spectra*, vol. 27, no. 3, pp. 797-815, 2011.
[15] F. Zareian and H. Krawinkler, "Assessment of probability of collapse and design for collapse safety," *Earthquake Engineering & Structural Dynamics*, vol. 36, no. 13, pp. 1901-1914, 2007.
[16] F. C. Filippou, T. N.Do, J. Cohen, and J. Chen. (2018) Resolution of Non-Convergence Issues in Seismic Response Analysis of Bridges. *PEER Center News*.
[17] J. W. Baker and C. Cornell, "A vector-valued ground motion intensity measure consisting of spectral acceleration and epsilon," *Earthquake Engineering & Structural Dynamics*, vol. 34, no. 10, pp. 1193-1217, 2005.
[18] H. Aslani and E. Miranda, "Probability-based seismic response analysis," *Engineering Structures*, vol. 27, no. 8, pp. 1151-1163, 2005.

